

Deconfounding the Effects of Resting State Activity on Task Activation Detection in fMRI

Burak Yoldemir¹, Bernard Ng², and Rafeef Abugharbieh¹

¹ Biomedical Signal and Image Computing Lab, UBC, Canada

² Parietal Team, INRIA Saclay, France

{buraky,rafeef}@ece.ubc.ca, bernardying@gmail.com

Abstract. Inferring brain activation from functional magnetic resonance imaging (fMRI) data is greatly complicated by the presence of strong noise. Recent studies suggest that part of the noise in task fMRI data actually pertains to ongoing resting state (RS) brain activity. Due to the sporadic nature of RS temporal dynamics, pre-specifying temporal regressors to reduce the confounding effects of RS activity on task activation detection is far from trivial. In this paper, we propose a novel approach that exploits the intrinsic task-rest relationships in brain activity for addressing this challenging problem. With an approximate task activation pattern serving as a seed, we first infer areas in the brain that are intrinsically connected to this seed from RS-fMRI data. We then apply principal component analysis to extract the RS component within the task fMRI time courses of the identified intrinsically-connected brain areas. Using the learned RS modulations as confound regressors, we re-estimate the task activation pattern, and repeat this process until convergence. On real data, we show that removal of the estimated RS modulations from task fMRI data significantly improves activation detection. Our results thus provide further support for the presence of continual RS activity superimposed on task fMRI response.

Keywords: activation detection, fMRI, resting state, task-rest interactions

1 Introduction

Functional magnetic resonance imaging (fMRI) has become a primary means for studying human brain activity. To map brain areas to function, the standard analysis approach models fMRI observations as a combination of expected temporal responses using a general linear model (GLM) [1]. However, the strong noise in fMRI data arising from confounds, such as scanner drifts, motion artifacts, and physiological effects, greatly hampers reliable detection of brain activation. Recent studies have shown that the brain is not idle in the absence of external stimulus [2]. Instead, spontaneous modulations in brain activity, referred to as resting state (RS) activity, are continually present [2]. Moreover, there is evidence indicating that RS activity actually persists during task performance [3]. Thus, part of the noise observed in task fMRI data in-

deed ascribes to ongoing RS activity. The frequency range at which RS activity resides is typically found to be between 0.01 to 0.1 Hz [2], which overlaps with the stimulus frequencies employed in most task-based fMRI studies. Thus, standard high pass filtering e.g. at 1/128 Hz, which is the default cutoff frequency in the SPM software, for removing temporal drifts in task fMRI data, would not account for ongoing RS modulations. Also, unlike task-evoked responses, which are time-locked to stimulus, the time at which RS activity peaks and troughs is difficult to predict. Hence, pre-specifying temporal regressors to model RS activity is non-trivial.

Albeit its seemingly sporadic temporal dynamics, RS activity is not random [2]. Rather, strong synchrony in RS modulations between specific brain areas has been observed in numerous studies [2]. In fact, many of the detected RS networks exhibit high resemblance to networks seen in task experiments [4]. Further supporting this finding is a recent work [5] that demonstrated enhanced sensitivity in task activation detection by incorporating an RS-connectivity prior. In addition, studies that jointly examined RS-fMRI and diffusion MRI data indicate an anatomical basis for RS activity [6, 7]. In particular, high anatomical connectivity typically predicts high functional connectivity [6, 7]. Thus, the spatial patterns of RS networks would presumably be constrained by the underlying fiber pathways [6, 7]. Taken together, these findings suggest that there is spatial structure in RS activity and that the spatial structure of ongoing RS activity during task would likely remain similar to that during rest [3].

To the best of our knowledge, the only previous work that attempted to tackle this challenging problem of RS activity removal from task fMRI data was by Fox et al. [3]. Specifically, the authors showed that for a right handed motor task, subtracting out fMRI signals in the right somatomotor cortex (RSC) from the left somatomotor cortex (LSC) significantly reduced inter-trial variability in fMRI response. The basis of this approach is twofold. First, the presence of coherent RS activity between the LSC and RSC is well established [8], and is assumed to persist during task performance. Second, right handed motor tasks typically activate only the LSC, thus signals in RSC would largely correspond to RS activity. Subtraction of signals in RSC from LSC would thereby remove the RS components within the task fMRI time courses of the LSC. However, not all tasks evoke only lateralized activation. Thus, simply subtracting signals in one side of the brain from the other side is not always suitable for removing RS modulations from task fMRI data.

In this paper, we propose a novel approach for RS activity removal in more general settings. The key challenge to this problem is that RS activity is internally-driven by the brain, as opposed to being evoked by external stimulus with known timing. It is thus not obvious how the temporal dynamics of RS modulations that occurred during task performance can be determined a priori. Representative time courses reflective of ongoing RS activity must hence be extracted from the task fMRI data itself. Since the brain comprises multiple networks [4], the RS modulations superimposed on the fMRI responses of the task-activated brain areas would be specific to the RS network in which these brain areas belong. Extracting RS activity from task fMRI data would thus require knowing the parts of the brain that are activated and their intrinsically-connected areas, which introduces a circular problem. To deal with this issue, we employ an iterative strategy in which we first apply seed-based analysis [8] with an

approximate task activation pattern being the seed to infer the intrinsically-connected brain areas from RS-fMRI data. Assuming the spatial structure of RS networks is sustained during task performance [3], we extract RS modulations from the task fMRI time courses of the identified brain areas and re-estimate the task activation pattern with the learned RS activity as confound regressors. On real fMRI data collected from 19 subjects undergoing a checkerboard-viewing task, we show that repeating this process to remove ongoing RS modulations from task fMRI data significantly improves task activation detection.

2 Proposed RS Activity Removal Approach

Motivated by the recent finding that RS activity contributes to the noise in task fMRI data [3], we propose a novel approach for removing such confounds to improve activation detection. Our approach consists of three steps, as summarized in Fig. 1.

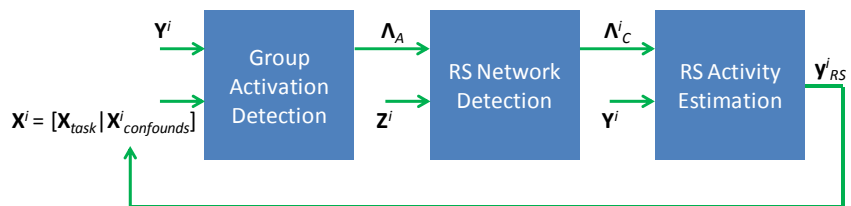


Fig. 1. Depiction of proposed RS activity removal approach. $\mathbf{X}^i = [\mathbf{X}_{task} | \mathbf{X}_{confounds}^i]$ is a regressor matrix, where \mathbf{X}_{task} corresponds to task regressors and $\mathbf{X}_{confounds}^i$ corresponds to confound regressors specific to subject i . \mathbf{Y}^i are the task fMRI time courses of subject i . Λ_A is the set of activated brain areas common across a group of subjects. \mathbf{Z}^i are the RS-fMRI time courses of subject i . Λ_C^i is the set of brain areas estimated to be intrinsically connected to Λ_A for subject i . \mathbf{y}_{RS}^i is the estimated RS activity time course of subject i , which is entered into \mathbf{X}^i as a confound regressor for re-estimating the group activation pattern Λ_A . The three steps: group activation detection, RS network detection, and RS activity estimation, are repeated until Λ_A stabilizes.

In brief, we first approximate the task activation pattern that is common across subjects using standard univariate analysis [1] (Section 2.1). With the detected activation pattern serving as a seed, we infer brain areas that are intrinsically-connected to this seed from RS-fMRI data of each subject [8] (Section 2.2). Assuming that the spatial structure of RS networks remains fixed during task [3], we apply principal component analysis (PCA) to extract the RS component from the task fMRI time courses of the identified intrinsically-connected brain areas (Section 2.3). The estimated RS modulations are then used as confound regressors to re-estimate the task activation pattern of the group, and this process is repeated until the detected activation pattern converges.

2.1 Seed Region Extraction

Our approach begins with the estimation of an approximate task activation pattern (i.e. without accounting for ongoing RS modulations). A standard general linear model (GLM) is first applied to compute the intra-subject activation effects [1]:

$$\mathbf{Y}^i = \mathbf{X}^i \boldsymbol{\beta}^i + \mathbf{E}^i, \quad (1)$$

where \mathbf{Y}^i is an $t \times d$ matrix containing the task fMRI time courses of d brain areas of subject i , $\mathbf{X}^i = [\mathbf{X}_{task} | \mathbf{X}_{confounds}^i]$ is an $t \times p$ matrix with \mathbf{X}_{task} corresponding to task regressors and $\mathbf{X}_{confounds}^i$ corresponding to confound regressors specific to subject i [1], $\boldsymbol{\beta}^i$ is an $p \times d$ activation effect matrix to be estimated, and \mathbf{E}^i is an $t \times d$ residual matrix. Due to the strong noise in task fMRI data, activation patterns estimated at the intra-subject level might be inaccurate [9]. Therefore, we opt to combine information across subjects in generating a group activation map, which is then used as a seed for identifying intrinsically-connected brain areas (Section 2.2). To infer group activation, we apply a max-t permutation test [10] on $\boldsymbol{\beta}^i$ of all subjects, which implicitly accounts for multiple comparisons and provides strong control over false detections. Group activation is declared at a p-value threshold of 0.05. We denote the set of detected brain areas as Λ_A .

2.2 RS Network Detection

With the detected group activation pattern taken as a seed, our goal is to identify brain areas that belong to the same RS network as the seed, so that we can extract RS modulations specific to this RS network. To proceed, we first average the RS-fMRI time courses within the detected activated brain areas in generating a seed time course for each subject. We then apply the standard seed-based analysis [8] to find brain areas intrinsically-connected to this seed for each subject i :

$$\mathbf{Z}_{\sim s}^i = \mathbf{z}_s^i \mathbf{w}^i + \boldsymbol{\Omega}^i, \quad (2)$$

where $\mathbf{Z}_{\sim s}^i$ is an $n \times (d - |\Lambda_A|)$ matrix containing the RS-fMRI time courses of all brain areas except those in Λ_A , $|\Lambda_A|$ is the number of brain areas in Λ_A , \mathbf{z}_s^i is an $n \times 1$ vector containing the seed time course, \mathbf{w}^i is an $1 \times (d - |\Lambda_A|)$ vector with each element reflecting the correlation between the seed and each brain area not in Λ_A , and $\boldsymbol{\Omega}^i$ is an $n \times (d - |\Lambda_A|)$ residual matrix. Statistical significance of each element of \mathbf{w}^i is declared at a p-value threshold of 0.05 with false discovery rate (FDR) correction [11] to account for multiple comparisons. FDR correction is used instead of max-t permutation test due to correlations between brain volumes at adjacent time points, which violates the independent sample assumption in max-t permutation test [10]. A max-t permutation test could be applied to identify brain areas that are significantly correlated with the seed at the group level. However, compared to task-based experiments, RS experiments are

less prone to motion artifacts, which constitute a major part of fMRI noise. Reliable RS networks could thus potentially be extracted at the intra-subject level. We hence opt to perform intra-subject seed-based analysis to retain subject-specific information. We denote the set of brain areas significantly correlated with the seed as Λ_C^i .

2.3 RS Activity Estimation and Removal

After finding the set of brain areas that is intrinsically-connected to the estimated task activation pattern for each subject i , the next step is to extract the RS components from the task fMRI time courses of these brain areas, which we denote as \mathbf{Y}_C^i . To target the specific frequency range at which RS activity resides, we first band-pass filter each column of \mathbf{Y}_C^i at cut-off frequencies of 0.01 and 0.1 Hz. Since the estimated task activation pattern is only an approximation without accounting for the confounding effects of RS activity, some intrinsically-connected brain areas might in fact be activated considering the resemblance between task and RS networks [4]. Thus, \mathbf{Y}_C^i might contain task signals. To remove the task-related response in \mathbf{Y}_C^i , we apply PCA through eigen-decomposition to separate \mathbf{Y}_C^i into task and non-task components:

$$\mathbf{C}^i = \mathbf{U}^i \mathbf{D}^i \mathbf{U}^{iT}, \quad (3)$$

where \mathbf{C}^i is the $d \times d$ covariance matrix of \mathbf{Y}_C^i , \mathbf{U}^i is an $d \times d$ matrix containing the eigenvectors of \mathbf{C}^i , and \mathbf{D}^i is an $d \times d$ matrix containing the eigenvalues of \mathbf{C}^i along the diagonal. The columns of \mathbf{U}^i are ordered such that the first column, \mathbf{U}_1^i , corresponds to the largest eigenvalue. To identify the task-related components, we compute the correlation between each column of \mathbf{U}^i and the task regressor. Statistical significance in correlation is declared at a p-value threshold of 0.05 with FDR correction. For the data examined in this work (Section 3), the task regressor is found to be most significantly correlated with \mathbf{U}_1^i . This high correlation between \mathbf{U}_1^i and the task stimulus, as shown in Fig. 1, signifies a definite need for task response removal from \mathbf{Y}_C^i . We remove the task components by reconstructing \mathbf{Y}_C^i with the significantly correlated columns of \mathbf{U}^i discarded. We note that other decomposition techniques, such as independent component analysis (ICA) [12], could be also used. We defer comparisons between various decomposition techniques for future work.

Denoting the reconstructed \mathbf{Y}_C^i as \mathbf{V}_{-task}^i , we take the mean of \mathbf{V}_{-task}^i over brain areas to generate a representative RS activity time course for each subject i , \mathbf{y}_{RS}^i , which we enter into (1) as a confound regressor to re-estimate the task activation pattern. This process is repeated until the group activation pattern Λ_A stabilizes.

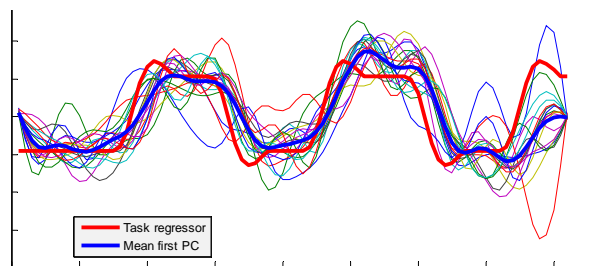


Fig. 1. Dominant principal component (PC) extracted from time courses of intrinsically-connected brain areas. The thick red and blue lines correspond to task regressor and mean dominant PC across subjects. Each thin line corresponds to the dominant PC of a single subject.

3 Materials

For testing our proposed RS activity removal approach, we used the publicly available Multiband Test-Retest Pilot Dataset, which was released as a part of the 1000 Functional Connectomes Project¹. Excluding subjects with missing brain volumes, the dataset comprises 19 subjects (14 men, 5 women, mean age 33.1 ± 13.2 years). Each subject performed a passive viewing task in which a checkerboard was displayed on a monitor for 20 s, with 20 s of rest interleaved between stimulus blocks. The total task duration was approximately 2.5 minutes. Task fMRI data were acquired with a TR of 1.4 s and a voxel size of 2 mm (isotropic). RS-fMRI data of 5 minutes duration were also collected with a TR of 2.5 s and a voxel size of 3mm (isotropic).

For each subject's RS-fMRI data, motion correction and spatial normalization were performed using SPM8. The voxel time courses were then bandpass filtered at cutoff frequencies of 0.01 and 0.1 Hz with white matter and cerebrospinal fluid confounds regressed out. In accordance with how the human brain is estimated to comprise ~ 500 functional regions [13, 14], we functionally divided the brain into 500 parcels as follows. First, we used the Freesurfer atlas to divide the brain into 112 anatomical regions. We then functionally subdivided each anatomical region into N_r parcels, where N_r is chosen based on the number of voxels within each anatomical region relative to the total number of voxels. Parcellation was performed by concatenating RS-fMRI voxel time courses across subjects and applying normalized cut [15] to the correlation matrix computed from the concatenated time courses. RS parcel time courses were then generated by averaging the RS-fMRI voxel time courses within each group parcel. For task fMRI data, similar preprocessing steps were performed, except a high-pass filter at 1/128 Hz was used to remove temporal drifts. Task fMRI time courses within each group parcel were averaged to compute task parcel time courses.

¹ The Multiband Test-Retest Pilot Dataset is available online at: http://fcon_1000.projects.nitrc.org/indi/pro/eNKI_RS_TRT/FrontPage.html

4 Results and Discussion

To validate our proposed approach, we compared applying the standard univariate analysis [1] with and without RS activity removal in detecting group activation. We denote these two cases as RSR and GLM, respectively. For increased group activation detection to be a legitimate validation criterion, strong control over false positive rate is critical. For this, we used the max-t permutation test [10] for both RSR and GLM, which implicitly accounts for multiple comparisons, provides strong control on false positive rate, and generates less conservative t-value thresholds than Gaussian random field theory and Bonferroni correction [10].

Fig. 2 shows the number of detected parcels for different p-value thresholds. For the same specificity, our approach provided higher detection sensitivity than GLM in general. To assess whether the increased detection was statistically significant, we employed a “parcel-label” permutation test. Specifically, for each permutation, we first randomly selected half of the parcels and exchanged the labels (i.e. active or non-active) assigned by RSR and GLM for each p-value threshold. We then computed the difference in the number of detected parcels with and without RS removal, which we denote as N_{diff} . This procedure was repeated 1000 times to generate a null distribution. The original N_{diff} was found to be greater than the 95th percentile of the null distribution for all corrected p-value thresholds within the typical range of [0.01, 0.05]. The detection improvement with RSR compared to GLM was thus statistically significant. We note that improvement in detection was observed even with just one iteration of RSR, and the detected activation pattern stabilized within two iterations, i.e. no more than a couple of parcels changing labels in subsequent iterations.

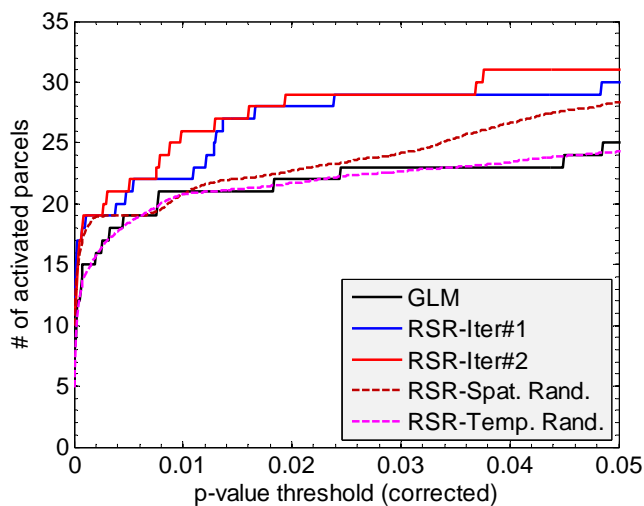


Fig. 2. Activation detection comparison. Number of parcels detected with significant activation vs. p-value thresholds.

To show that there is specific temporal structure in the estimated RS activity time courses that gave rise to the observed detection improvement, we applied RSR on temporally-permuted RS activity time courses 100 times. The average number of detected parcels over the 100 permutations (RSR-Temp. Rand. in Fig. 2) was found to be similar to that of GLM. The difference in detection performance between RSR and RSR-Temp. Rand. was statistically significant based on the parcel-label permutation test with a threshold set at the 95th percentile of the null distribution. Our results thus indicate that there is certain temporal structure in the estimated RS activity time courses that is critical for successful RS activity removal.

Since the brain comprises multiple networks [4], not all parcels would contain the same RS modulations as those superimposed on the underlying task activated brain areas. To illustrate this point, we applied RSR with RS modulations extracted from N_c randomly selected parcels (excluding parcels identified by RSR), where N_c is the number of intrinsically-connected brain areas originally determined with RSR. The average number of detected parcels over 100 random subsets of parcels (RSR-Spat. Rand. in Fig. 2) was found to be similar to that of GLM for p-value thresholds between 0 and 0.02, and modestly better than GLM for p-value thresholds above 0.02. We suspect the increased detection arises from how some parcels might be intrinsically-connected to the task-evoked brain areas, but the estimated correlations were declared not significant due to noise. Such parcels would contain RS modulations common to the task activation pattern, hence the increased activation detection observed. Nevertheless, the increase was not statistically significant based on the parcel-label permutation test with a threshold set at the 95th percentile of the null distribution.

Qualitatively, RSR additionally detected brain areas adjacent to those found by GLM (Fig. 3). More bilateral activation was also found with RSR. The detected brain areas lie within the primary visual cortex and the extrastriate cortex, which are known to pertain to visual checkerboard stimulus [16, 17], hence confirming our results.

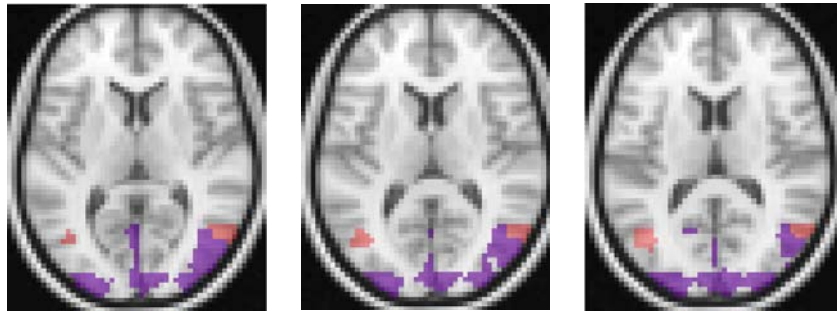


Fig. 3. Detected activation patterns. Three axial slices shown. Parcels detected at p-value < 0.05 (corrected). Red = detected by RSR only. Purple = detected by both GLM and RSR.

5 Conclusions

We proposed a novel approach for the estimation and removal of continual RS activity in task fMRI data. Exploiting how the spatial structure of RS networks are constrained by the underlying fiber pathways hence would remain similar during task performance, our approach first extracts RS modulations from task fMRI time courses within brain areas that are significantly correlated with an approximate task activation pattern at rest. The estimated RS modulations are then entered into a GLM as confound regressors to model the effects of RS activity. Applying our approach on real data resulted in statistically significant improvement in task activation detection. In agreement with the seminal work by Fox et al. [3], our results indicate that RS activity also contributes to the noise seen in task fMRI data, in contrast to the traditional belief that only scanner artifacts, head motions, and physiological confounds contribute to fMRI noise. It is thus important to model RS activity in task fMRI studies.

References

1. Friston, K.J., Holmes, A.P., Worsley, K.J., Poline, J.B., Frith, C.D., Frackowiak, R.S.J.: Statistical Parametric Maps in Functional Imaging: A General Linear Approach. *Hum. Brain Mapp.* 2, 189–210 (1995)
2. Fox, M.D., Raichle, M.E.: Spontaneous Fluctuations in Brain Activity Observed with Functional Magnetic Resonance Imaging. *Nat. Rev. Neurosci.* 8, 700–711 (2007)
3. Fox, M.D., Snyder, A.Z., Vincent, J.L., Raichle, M.E.: Intrinsic Fluctuations within Cortical Systems Account for Intertrial Variability in Human Behaviour. *Neuron* 56, 171–184 (2007)
4. Smith, S.M., Fox, P.T., Miller, K.L., Glahn, D.C., Fox, P.M., Mackay, C.E., Filippini, N., Watkins, K.E., Toro, R., Laird, A.R., Beckmann, C.F.: Correspondence of the Brain's Functional Architecture During Activation and Rest. *Proc. Natl. Acad. Sci.* 106, 13040–13045 (2009)
5. Ng, B., Abugharbieh, R., Varoquaux, G., Poline, J.B., Thirion, B.: Connectivity-informed fMRI Activation Detection. In: Fichtinger, G., Martel, A., Peters, T. (eds.) MICCAI 2011. LNCS, vol. 6892, pp. 285–292, Springer, Heidelberg (2011)
6. Honey, C.J., Thivierge, J.P., Sporns, O.: Can Structure Predict Function in the Human Brain? *NeuroImage* 52, 766–776 (2010)
7. Damoiseaux, J.S., Greicius, M.D.: Greater than the Sum of its Parts: A Review of Studies Combining Structural Connectivity and Resting-state Functional Connectivity. *Brain Struct. Funct.* 213, 525–533 (2009)
8. Biswal, B., Yetkin, F.Z., Haughton, V.M., Hyde, J.S.: Functional Connectivity in the Motor Cortex of Resting Human Brain Using Echo-planar MRI. *Magn. Reson. Med.* 34, 537–541 (1995)
9. Ng, B., Hamarneh, G., Abugharbieh, R.: Modeling Brain Activation in fMRI Using Group MRF. *IEEE Trans. Med. Imaging* 31, 1113–1123 (2012)
10. Nichols, T., Hayasaka, S.: Controlling the Familywise Error Rate in Functional Neuroimaging: A Comparative Review. *Stat. Methods Med. Research* 12, 419–446 (2003)
11. Benjamini, Y., Hochberg, Y.: Controlling the False Discovery Rate: A Practical and Powerful Approach to Multiple Testing. *J. Royal Stat. Soc. Series B* 57, 125–133 (1995)

12. McKeown, M.J., Makeig, S., Brown, G.G., Jung, T.-P., Kindermann, S.S., Bell, A.J., Sejnowski, T.J.: Analysis of fMRI Data by Blind Separation into Independent Spatial Components. *Hum. Brain Mapp.* 6, 160–188 (1998)
13. Tucholka, A., Thirion, B., Perrot, M., Pinel, P., Mangin, J.F., Poline, J.B.: Probabilistic Anatomic-functional Parcellation of the Cortex: How Many Regions? In: Metaxas, D., Axel, L., Fichtinger, G., Szekely, G. (eds.) *MICCAI 2008*. LNCS, vol. 5242, Springer, Heidelberg (2008)
14. Thyreau, B., Thirion, B., Flandin, G., Poline, J.B.: Anatomic-functional Description of the Brain: A Probabilistic Approach. In: *31st IEEE International Conference on Acoustics, Speech, and Signal Processing*, pp. 1109–1112 (2006)
15. Van Den Heuvel, M., Mandl, R., Hulshoff Pol, H.: Normalized Cut Group Clustering of Resting-state fMRI Data. *PLoS ONE* 3, e2001 (2008)
16. Liu, Z., Zhang, N., Chen, W., He, B.: Mapping the Bilateral Visual Integration by EEG and fMRI. *NeuroImage* 46, 989–997 (2009)
17. Clare, S.: Magnetic Resonance Imaging of Brain Function. *Methods Enzymol.* 385, 134–148 (2004)